JCB Article

BMPs signal alternately through a SMAD or FRAP–STAT pathway to regulate fate choice in CNS stem cells

Prithi Rajan, David M. Panchision, Laura F. Newell, and Ronald D.G. McKay

Laboratory of Molecular Biology, National Institute of Neurological Disorders and Stroke, National Institutes of Health, Bethesda, MD 20892

The ability of stem cells to generate distinct fates is critical for the generation of cellular diversity during development. Central nervous system (CNS) stem cells respond to bone morphogenetic protein (BMP) 4 by differentiating into a wide variety of dorsal CNS and neural crest cell types. We show that distinct mechanisms are responsible for the generation of two of these cell types, smooth muscle and glia. Smooth muscle differentiation requires BMP-mediated Smad1/5/8 activation and predominates where local cell density is low. In contrast, glial differentiation predominates at high local densities in response to BMP4 and is specifically blocked by a dominant-negative mutant Stat3. Upon BMP4 treatment, the serine-threonine kinase FKBP12/rapamycin-associated protein (FRAP), mammalian target of rapamycin (mTOR), associates with Stat3 and facilitates STAT activation. Inhibition of FRAP prevents STAT activation and glial differentiation. Thus, glial differentiation by BMP4 occurs by a novel pathway mediated by FRAP and STAT proteins. These results suggest that a single ligand can regulate cell fate by activating distinct cytoplasmic signals.

Introduction

Recent work suggests that the wide arrays of cell types that can be generated during development depend critically on the actions of extracellular signals on multipotent precursors (Dorsky et al., 2000; Panchision and McKay, 2002; Zhu and Emerson, 2002). Isolated central nervous system (CNS)* stem cells can be exposed to novel environments to differentiate into both CNS fates as well as non-CNS fates including skeletal muscle and hematopoetic derivatives (Valtz et al., 1991; Bjornson et al., 1999; Galli et al., 2000). Similarly, cell populations enriched for hematopoietic stem cells can differentiate into hepatocytes, cardiomyocytes, and skeletal muscle cells (Gussoni et al., 1999; Jackson et al., 1999; Lagasse et al., 2000). These results have provoked a great deal of interest in the fundamental mechanisms controlling cell fate choice and in the potential for exploiting this knowledge for new therapies.

Cultured stem cells are increasingly used to analyze mechanisms of cellular differentiation because of the easy access to large numbers of self-renewing cells that exhibit rapid, controlled and reproducible differentiation. We have previously shown that CNS stem cells isolated from the embryonic rodent brain can be expanded in large numbers using the mitogen basic FGF (bFGF) to maintain self-renewal (Vicario-Abejon et al., 1995; Johe et al., 1996). Upon bFGF withdrawal, these cells will differentiate into the three characteristic CNS lineages: neurons, astrocytes, and oligodendrocytes (Johe et al., 1996). Furthermore, they can be efficiently redirected to specific CNS fates by the addition of single extracellular factors such as platelet-derived growth factor, triiodothyronine, and ciliary neurotrophic factor (CNTF) (Johe et al., 1996). CNTF rapidly and robustly instructs CNS stem cells to a glial fate and requires the actions of Stat3 (Bonni et al., 1997; Rajan and McKay, 1998).

Bone morphogenetic proteins (BMPs) have diverse actions on the fate choice and differentiation of CNS stem cells during development. BMPs induce dorsal precursor fates, including roof plate, choroid plexus epithelium, and neural crest (Shah et al., 1996; Liem et al., 1997; Sela-Donenfeld and Kalcheim, 1999; Panchision et al., 2001), and induce apoptosis or terminal differentiation in the developing neural tube (Graham et

P. Rajan and D.M. Panchision contributed equally to this work.

Address correspondence to Ronald D.G. McKay, 36 Convent Drive, MSC 4092, Bethesda, MD 20892. Tel.: (301) 496-6574. Fax: (301) 402-1340. E-mail: mckay@codon.nih.gov

P. Rajan's present address is Psychiatric Genomics, Inc., 19 Firstfield Road, Gaithersburg, MD 20878.

*Abbreviations used in this paper: bFGF, basic FGF; BMP, bone morphogenetic protein; BMPR-IA, BMP receptor type one A; CNS, central nervous system; CNTF, ciliary neurotrophic factor; EMSA, electrophoretic mobility shift assay; FRAP, FKBP12/rapamycin-associated protein; FRB, FKBP12-rapamycin binding; GFAP, glial fibrillary acidic protein; SMA, smooth muscle α-actin.

Key words: bone morphogenetic protein; stem cell; SMAD; STAT; mammalian FRAP

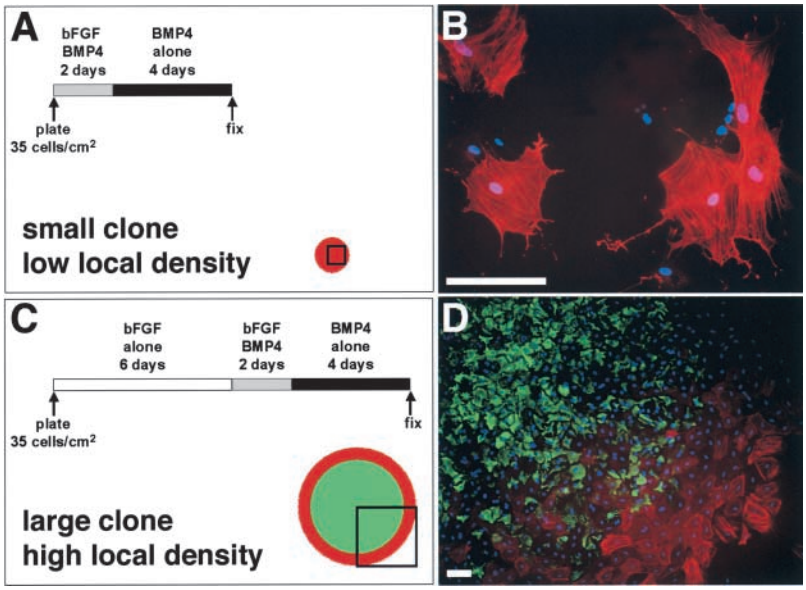

Figure 1. **BMP4-treated cortical stem cells will differentiate into smooth muscle or glia depending on local density.** (A) Low-density treatment schedule. E14.5 cortical stem cells were plated at clonal density (35 cell/cm^2) and instructed immediately with BMP4 along with bFGF (10 ng/ml each) for 2 d, followed by differentiation with BMP4 alone for 4 d. (B) This results in small clones with a low local cell density and differentiation into almost exclusively SMA$^+$ smooth muscle. (C) High-density treatment schedule. E14.5 cortical stem cells were plated at clonal density, expanded in bFGF to increase local cell density, and then instructed with BMP4 along with bFGF for 2 d, followed by differentiation with BMP4 alone for 4 d. (D) This results in clones with a high central density (GFAP$^+$ glia) and a low density around the periphery (SMA$^+$ smooth muscle). These regions meet at a boundary of interspersed smooth muscle, glia, and cells with a transitional morphology that have weak or absent staining for these markers. Rectangles in cartoon clones indicate area shown in fluorescent images. Bars, 100 μm.

al., 1996; Furuta et al., 1997; Li et al., 1998; Panchision et al., 2001). BMP stimulation of CNS precursors in vitro leads to differentiation into CNS neurons (Mabie et al., 1999) and glia (Gross et al., 1996) and neural crest derivatives such smooth muscle, peripheral neurons, and Schwann cells (Mujtaba et al., 1998; Molne et al., 2000; Panchision et al., 2001). These diverse responses to BMPs may be due to (a) other signals that modulate the response to BMPs (Sun et al., 2001; White et al., 2001) and/or (b) the activation of different BMP signal transduction pathways. Here we show that the differentiation of two distinct cell fates, smooth muscle and glia, is modulated by density and is controlled by alternative use of two distinct cytoplasmic BMP pathways.

Results

Local density affects stem cell fate choice in response to BMPs

BMPs are known to instruct CNS stem cells to dorsal fates, such as neural crest, and to subsequently differentiate these dorsalized precursors to peripheral neurons, Schwann cells, and smooth muscle (Mujtaba et al., 1998; Molne et al., 2000; Panchision et al., 2001). In response to BMP2 or BMP4 treatment, CNS stem cells at low local density gave rise to a high proportion of smooth muscle cells, as measured by smooth muscle α-actin (SMA) staining. The generation of smooth muscle was more efficient with increasing concentrations of BMP4 (Table I). At higher local densities, stem cells gave rise to high proportions of glia, as measured by glial fibrillary acidic protein (GFAP) (Fig. 1).

To determine whether these two fates can arise from the same cell, we plated cortical stem cells at clonal density (35 cells/cm^2) in the presence of bFGF as a mitogen. The cells were treated with BMP4 for 2 d, starting either immediately upon plating (Fig. 1 A) or after 6 d of bFGF expansion (Fig. 1 C), and allowed to terminally differentiate in the presence of BMP4 alone. Cultures that received BMP treatment immediately upon plating efficiently and uniformly generated small, sparse clones of ∼2–30 cells that were almost exclusively SMA$^+$ (Fig. 1 B; Table I). In cultures that received 6 d of expansion in bFGF alone, clones had ∼180–330 cells with an average cell cycle time of ∼18 h. At the initiation of BMP treatment, the center of each clone had reached a high local density while the periphery of the clone remained sparse. By the end of BMP treatment, the center of each clone was almost exclusively GFAP$^+$ glia while the periphery of each clone was almost exclusively SMA$^+$ smooth muscle (Fig. 1 D). The boundary between the dense core and the sparse periphery of clones consisted of a mixture of glia and smooth muscle, as well as GFAP$^-$SMA$^-$ or GFAP^{low}SMA^{low} cells that had morphologies intermediate between the sheet-like morphology of smooth muscle and the process-bearing morphology of the glia.

Neurons were also generated in both low- and high-density cultures, but in the absence of additional survival factors, the BMP-generated neurons usually died during differentiation. Thus, all clones in these BMP-treated cultures consisted predominantly of smooth muscle and glia. In contrast, stem cell clones grown to either low or high local density in the absence of BMP treatment generated only CNS neurons, astrocytes,

Table I. **Efficiency of smooth muscle differentiation in low-density culture**

BMP4	Clone size	Percent SMA$^+$ cells
ng/ml		
0	mass culture	0
1	mass culture	22.2 ± 14.0
5	mass culture	55.3 ± 14.3
10	mass culture	61.0 ± 21.7
20	mass culture	81.5 ± 6.2
10	1–5 cells	74.2 ± 6.8
10	6–10 cells	85.9 ± 6.9

For mass culture, cells were plated at 3,500 cells/cm^2 and immediately treated with BMP4 for 2 d with mitogen and 4 d after mitogen withdrawal. For clonal analysis, cells were plated at 35 cells/cm^2 and immediately treated with 10 ng/ml BMP4 for 2 d with mitogen and 4 days after mitogen withdrawal. No GFAP$^+$ cells were seen in these clones. Mean ± SEM; n = 4 for mass culture, n = 32 for 1–5 cell clones, and n = 9 for 6–10 cell clones.

Table II. **Effect of STAT or SMAD inhibition on BMP4-induced differentiation**

Transfection	Markers expressed	Percent cells coexpressing
dnStat3–FLAG	$FLAG^+/GFAP^+$	12.7 ± 4.9
	$FLAG^+/SMA^+$	85.2 ± 8.9
Smad7–HA	$HA^+/GFAP^+$	77.1 ± 12.5
	HA^+/SMA^+	15.6 ± 5.8

Cells were plated at 3,500 cells/cm^2, cultured with mitogen for 1 d before transfection and 3 d after transfection, and then treated with 10 ng/ml BMP4 for 3 d with mitogen and 3 d after mitogen withdrawal (see Materials and methods). Mean ± SEM, $n = 4$.

and oligodendrocytes, as reported in previous studies (Johe et al., 1996). This indicates that the BMP-induced generation of neural crest derivatives, such as smooth muscle (Table I), is an efficient response of cortical stem cells and not of any contaminating cell type. On the basis of these observations, we sought to determine how this difference in cell density affects the fate choice of stem cells in response to BMPs.

BMP regulates smooth muscle and glial fates by signaling through the SMAD and STAT pathways, respectively

BMPs generate many responses by activating the SMAD family of DNA binding proteins (Miyazono, 1999). Transient transfection assays were used to determine if SMAD activation was necessary for generation of either or both of the fates. Cells were transfected with a construct that constitutively expresses high levels of HA-tagged Smad7, an endogenous inhibitory SMAD that functions as a dominant negative (Souchelnytskyi et al., 1998; Ishisaki et al., 1999). The transfected protein was allowed to express for 3 d, after which BMP treatment was initiated. Of all HA–Smad7-transfected cells, 77% differentiated into glia whereas <16% differentiated into smooth muscle (Table II).

Previous work has shown that STAT activation is required for CNTF-induced astrocytic differentiation of CNS stem cells (Bonni et al., 1997; Rajan and McKay, 1998). We sought to determine if BMP-mediated glial differentiation was also dependent on STAT activation by transfecting stem cells with a FLAG-tagged dominant-negative Stat3 followed by BMP treatment. Of all cells transfected with dominant-negative Stat3 (Horvath et al., 1995), <13% differentiated into glia whereas 85% differentiated into smooth muscle in response to BMP4 (Table II). This result suggests that SMAD signaling is required for smooth muscle but not glial differentiation, whereas STAT signaling is required for glial but not smooth muscle differentiation.

These data suggest that smooth muscle and glial fates are independently controlled by SMAD and STAT activation, respectively. We verified the biochemical activation of SMAD proteins by performing immunoblotting assays with an antibody recognizing the phosphorylated forms of Smad1, 5, and 8 (Faure et al., 2000) on whole cell extracts prepared after a 1-h factor treatment. Although bFGF and CNTF each have strong proliferative and differentiative effects on stem cells (Johe et al., 1996; Rajan and McKay, 1998), they had no effect on the activation of Smad1/5/8 (Fig. 2 A). In contrast, BMP4 robustly activated Smad1/5/8 in both low- and high-density cultures (Fig. 2 A, lanes 3 and 6). This activation occurred within 30 min and continued beyond 4 h of BMP4 treatment (Fig. 2 B).

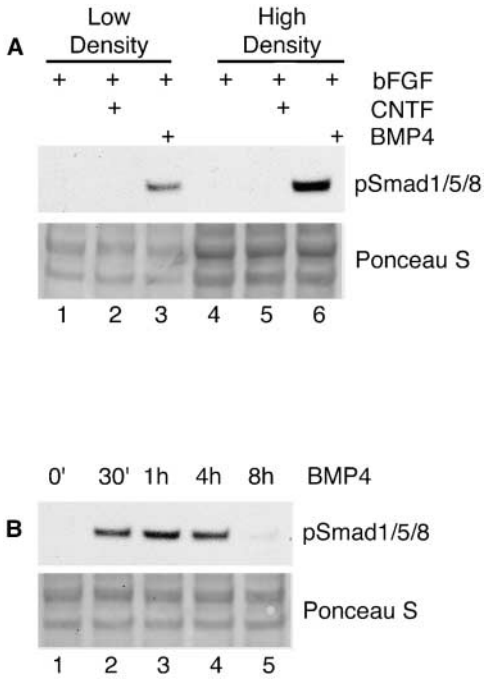

Figure 2. **BMP4 causes SMAD activation in both low- and high-density stem cell cultures.** Cells were treated with bFGF ± CNTF or BMP4 (10 ng/ml each) for 1 h. Normalized whole cell extracts were used for Western blot analysis with an anti-phosphoSMAD antibody recognizing activated Smad1, 5, and 8 (47 kD for Smad1 and 5; 40 kD for Smad8). (A) BMP4 treatment causes SMAD activation in both low- (lane 3) and high-density (lane 6) cultures. Control (lanes 1 and 4) or CNTF-treated (lanes 2 and 5) stem cells have no SMAD activation. (B) Time course of SMAD phosphorylation during BMP4 (10 ng/ml) ± bFGF (10 ng/ml) treatment of high-density cultures. BMP4 causes SMAD activation within 30 min (lane 2) that decreases at 8 h (lane 6). The lower panels of both figures show a Ponceau S staining of the nitrocellulose filter to demonstrate normalized loading of proteins across all lanes.

We verified STAT activation by electrophoretic mobility shift assay (EMSA), which measures the extent of binding of phosphorylated STAT proteins to a DNA oligonucleotide containing a specific recognition site. As we have previously shown (Rajan and McKay, 1998), the principal band consisted of a Stat3 homodimer complex with the oligonucleotide (Fig. 3 A, arrow), whereas the fainter band below it consisted of Stat3/Stat1 heterodimer complexes with the oligonucleotide. We found that basal levels of Stat3 activation were greater in high-density versus low-density cultures (Fig. 3, lanes 1 and 4). As expected, CNTF treatment dramatically increased Stat3 activation in both low- and high-density cultures (Fig. 3, lanes 2 and 5). BMP4 treatment had no effect on Stat3 activation in low-density cultures but activated Stat3 in high-density cultures (Fig. 3, lanes 3 and 6). These results indicate that although BMP4 activates SMADs in both low- and high-density cultures, it activates STATs only in high-density cultures that have higher basal levels of STAT activation and that give rise to glia. They also suggest the presence of a density-mediated signal that causes STAT activation.

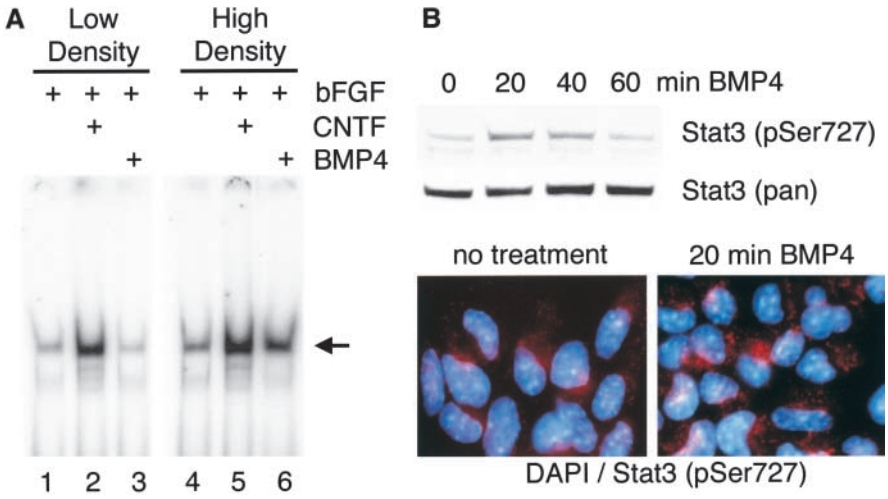

Figure 3. **BMP4 causes STAT activation only in high-density stem cell cultures.** (A) Cells were treated with bFGF ± CNTF for 1 h or BMP4 for 8 h (10 ng/ml each). Nuclear extracts were subjected to EMSA analysis using a ^{32}P-radiolabeled STAT binding site (double-stranded oligonucleotide) to measure STAT activation. Basal (bFGF treated only) levels of STAT binding are minimal in low-density cultures (lane 1) but are increased in high-density cultures (lane 4). CNTF treatment causes a strong increase in STAT binding in both low- (lane 2) and high-density (lane 5) cultures. BMP4 treatment of low-density cultures (lane 3) has no effect on STAT binding, whereas BMP4 treatment of high-density cultures (lane 6) causes increased STAT binding. The arrow marks complexes of Stat3 homodimers with STAT binding site oligonucleotides. The fainter bands below are complexes of Stat1 and Stat3 heterodimers with STAT binding site oligonucleotides. (B, top) Cortical stem cells were treated with BMP4 for 20, 40, or 60 min at 10 ng/ml, denaturing extracts prepared and analyzed on SDS-PAGE gels. The immunoblot was probed sequentially with antibodies specific for Stat3 phosphorylated on Ser727 and panStat3 for total levels of Stat3. BMP causes phosphorylation of Stat3 on Ser727, as seen in the top band of the figure. (B, bottom) Mouse cortical stem cells were cultured as described in the Materials and methods section and treated with BMP4 for 20 min before fixation. Cells were then stained with an antibody specific to the phosphor-ser727 Stat3 protein and viewed by indirect immunofluorescence. The DAPI staining is blue, and pser727Stat3 staining is red.

We performed immunoblots with an antibody specific to Stat3 phosphorylated on serine 727 (ser727) to verify BMP-mediated phosphorylation at this site (Fig. 3 B), which is one of the activation events that Stat3 undergoes (Zhang et al., 1995). Phosphorylation of ser727 was increased at 20 min after exposure to BMP4 and this elevation was long lasting. We also performed immunocytochemistry for phospho-ser727 Stat3 on mouse stem cell cultures that were treated with BMP4 (Fig. 3, C and D). Mouse cortical stem cells were seeded at 2,500 cells/cm^2, expanded for 5 d, and treated with 10 ng/ml BMP4 before fixation. Elevated levels of phospho-ser727 Stat3–specific staining were seen in cultures treated with BMP4, indicated by the increased red staining in Fig. 3 D. These data indicate that BMP4 causes activation of STAT proteins in stem cells and specifically phosphorylates Stat3 at ser727.

Maximal activation of STAT proteins by BMP was seen at 8 h. This treatment is prolonged when compared with CNTF, which causes maximal STAT activation at 15 min to 1 h. The long time required for BMP4 to activate STAT proteins suggests that some intermediary signal, perhaps a CNTF-like activity, becomes transcriptionally activated and that this is responsible for the activation of Stat3. We tested this possibility by treating the stem cells with the transcriptional inhibitor α-amanitin, which acts as a competitive inhibitor of RNA polymerase II (Wieland and Faulstich, 1978). Cotreatment of stem cells with α-amanitin did not block BMP4-mediated Stat3 binding (Fig. 4, compare lanes 4 and 5 with 9 and 10). These results make it unlikely that Stat3 activation requires a transcriptionally induced intermediate and instead suggests that BMP4 activates Stat3 directly through cytoplasmic signaling.

BMP4 induces glial fate through FRAP–Stat3

As there are no known mechanisms linking BMPs to STAT activation, we sought to determine the pathway by which this occurs. Previous studies showed that TGFβ receptors bind to the immunophilin FKBP12, which prevents SMAD activation in the absence of ligand binding (Chen et al., 1997; Stockwell and Schreiber, 1998). We performed coimmunoprecipitation experiments to see if FKBP12 binds BMP receptors in our stem cells. Nondenaturing cell extracts were immunoprecipitated with an antibody to FKBP12, and the complexes were analyzed on immunoblots

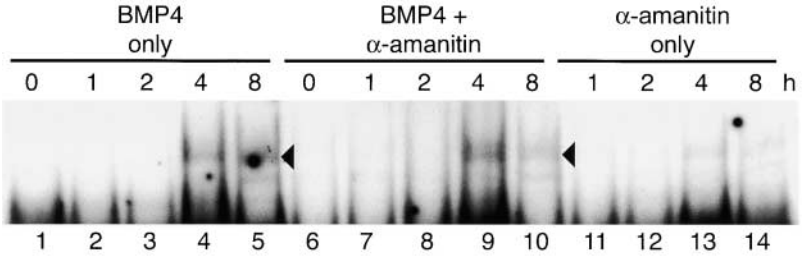

Figure 4. **BMP4-mediated activation of Stat3 does not require transcription.** Cortical stem cells were expanded in mass culture to high local density using bFGF (10 ng/ml) and then treated with 10 ng/ml BMP4 for the time points indicated in the absence (lanes 1–5) or presence (lanes 6–10) of 5 μg/ml α-amanitin. Control samples were treated with α-amanitin alone (lanes 11–14). Nuclear extracts were subjected to EMSA analysis using a ^{32}P-radiolabeled STAT binding site (double-stranded oligonucleotide) to measure STAT activation. Inhibition of transcription with α-amanitin does not prevent Stat3 binding in response to BMP4.

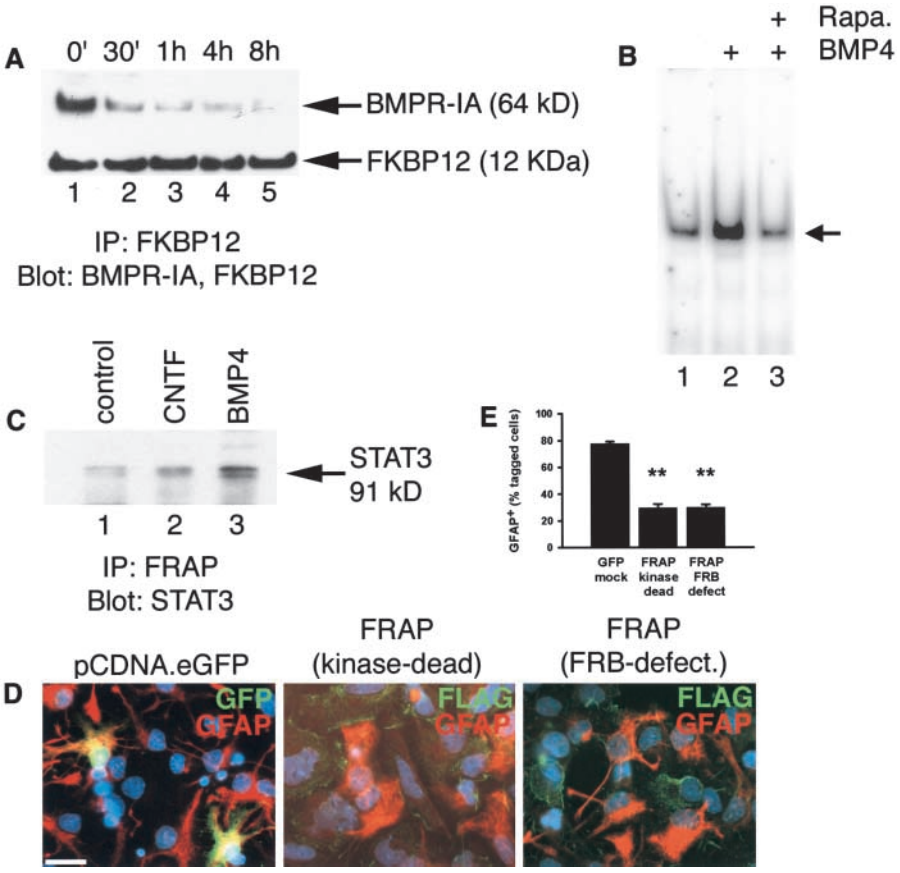

Figure 5. **BMP4-mediated activation of Stat3, and glial differentiation, requires FRAP.** (A) BMP4 causes dissociation of BMPR-IA and FKBP12. Cells were treated with BMP4 (10 ng/ml) for the duration of 30 min to 8 h, control sample was treated with bFGF for 8 h. Normalized, nondenatured whole cell lysates were immunoprecipitated with anti-FKBP12 before Western blot analysis using anti–BMPR-IA. BMP4 treatment causes a dissociation of BMPR-IA–FKBP12 complexes (arrow indicates 64-kD band). The lower panel shows the levels of FKBP12 in the immunoprecipitated complexes across all lanes. (B) BMP-mediated STAT activation is blocked by rapamycin. High-density stem cell cultures with enhanced STAT binding (lane 1) showed a further increase in STAT binding after BMP4 (10 ng/ml) treatment for 9 h (lane 2). Pretreatment with rapamycin for 12 h before BMP4 addition blocked further Stat3 binding (lane 3). (C) BMP4 treatment causes increased complex formation between FRAP and Stat3. Cells were treated with bFGF alone or with CNTF for 15 min or BMP4 for 4 h (10 ng/ml each). Note that 15 min represents the time of maximal Stat3 activation by CNTF. Normalized, nondenatured whole cell lysates were immunoprecipitated with anti-FRAP before Western blot analysis using anti-Stat3. Arrow indicates 91-kD band. Estimation of the levels of FRAP in the immunoprecipitated complexes could not be performed under the conditions optimal for Stat3 detection because FRAP is a substantially larger protein, 287 kD. (D) Activated FRAP is required for BMP-mediated glial differentiation. Cortical stem cells were transfected with NH_2-terminal FLAG-tagged dominant-negative FRAP mutants, Asp2357Glu, which is kinase dead, and Trp2027Phe, which is FRB defective. Cells were transfected for 3 h, treated with BMP4 in the presence of bFGF (both 10 ng/ml) for 2 d and BMP4 alone for 4 d, and then fixed and stained for GFAP and FLAG. Cells were counted by indirect immunofluorescence, and those expressing GFAP were calculated as a percentage of cells expressing FLAG protein. Control cultures were transfected with a GFP-expressing plasmid, which had no effect on BMP-mediated glial differentiation. (E) 80% of GFP-positive cells coexpress GFAP, whereas 25% of mutant FRAP–expressing cells coexpress GFAP, indicating that dominant-negative FRAP inhibits BMP-mediated GFAP expression. Mean $GFAP^+$ cells as a percentage of total transfected cells, $^{**}P < 0.001$. Bar, 20 μm.

with an antibody to BMP receptor type one A (BMPR-IA). We found that FKBP12 complexed with BMPR-IA in CNS stem cells, and that this complex dissociated when cells were treated with BMP4 (Fig. 5 A). The complex almost completely dissociated by 8 h after BMP4 treatment, when compared with the control, i.e., bFGF alone.

FKBP12 is a 12-kD protein that complexes with the immunosuppressant macromolecules rapamycin and FK506. Specifically, FKBP12 complexes with rapamycin to block the actions of the serine-threoine kinase FKBP12/rapamycin-associated protein (FRAP), mammalian target of rapamycin (mTOR) (Choi et al., 1996; Kuruvilla and Schreiber, 1999). EMSA assays were performed on stem cells treated for 9 h with BMP4 in the presence or absence of a pretreatment of rapamycin. We found that rapamycin blocked the BMP4-mediated activation of Stat3 in high-density cultures as measured by EMSA (Fig. 5 B). These observations implicate FRAP as the mediator of STAT activation in high-density cultures.

The observations that BMP-mediated activation is blocked by rapamycin and the correlated release of FKBP12 from the BMP receptor implicate FRAP as the mediator of STAT activation. A previous study has shown that FRAP can phosphorylate STAT proteins in response to CNTF (Yokogami et al., 2000). As this would involve direct interaction between FRAP and Stat3, we determined if BMP signaling increases complex formation between the two proteins. FRAP was immunoprecipitated from nondenaturing cell extracts, and the immunoprecipitated proteins were subsequently immunoblotted with an anti-Stat3 antibody. BMP treatment of CNS stem cells led to increased interaction of FRAP and Stat3 proteins by coimmunoprecipitation, greater than that seen with CNTF (Fig. 5 C). The binding of FRAP to Stat3 in response to BMP stimulation (Fig. 5 C) and the inhibition of Stat3 activation by rapamycin (Fig. 5 B) suggest that BMP4 activates Stat3 via a FRAP-mediated pathway.

As more direct evidence that FRAP is instrumental in mediating STAT activation, and hence glial differentiation, downstream of BMP, we determined the effect of two dominant-negative forms of FRAP on BMP-mediated astrocytic differentiation. The Trp2027Phe point mutation renders

FRAP defective in the FKBP12-rapamycin binding (FRB) domain, whereas Asp2357Glu point mutation deletes the kinase function of FRAP (Vilella-Bach et al., 1999). Both the constructs we have used are NH_2-terminal FLAG tagged. About 25% of stem cells transfected with the dominant-negative forms of FRAP differentiate into glia upon BMP treatment (Fig. 5, D and E), whereas in a control transfection with a GFP construct under identical experimental conditions, 80% of the culture differentiated into glia. These data indicate that FRAP activation is required for BMP-mediated glial differentiation.

BMP4-induced glial differentiation is rapamycin sensitive, whereas smooth muscle differentiation is rapamycin insensitive

We additionally looked at rapamycin inhibition of FRAP on fate choice. Stem cells that received no treatment before mitogen withdrawal generated glia with weak to moderate GFAP staining and an immature morphology (Fig. 6 A). Stem cells that received CNTF before mitogen withdrawal generated intensely stained $GFAP^+$ cells with a mature, stellate astrocytic morphology (Fig. 6 B), as described previously (Johe et al., 1996; Rajan and McKay, 1998). Treatment with BMP4 before mitogen withdrawal generated glia with strong GFAP staining and distinctly flattened morphology (Fig. 6 C). Stem cells that received BMP4 and rapamycin showed a dramatically reduced number of $GFAP^+$ cells, even in areas with high local density (Fig. 6 D). Additionally, we treated stem cells with FK506, another drug that complexes with FKBP12 but inhibits the phosphatase calcineurin (Abraham and Wiederrecht, 1996). We found that FK506 had no effect on the generation of glia by BMP4 (Fig. 6 E).

We counted cells in the transitional zones that give rise to both glia and smooth muscle in medium- and high-density

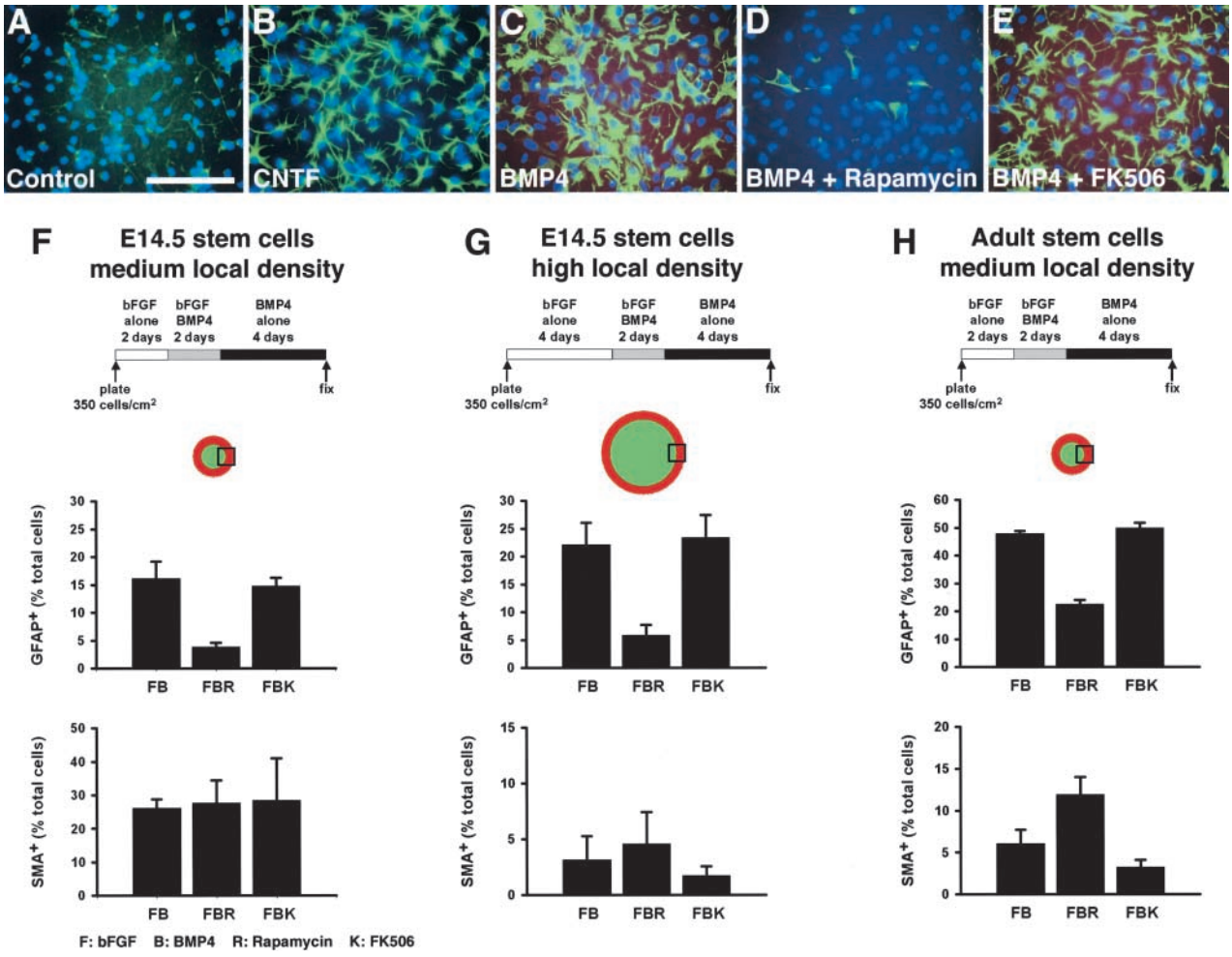

Figure 6. **BMP4-mediated glial differentiation is rapamycin sensitive, whereas smooth muscle differentiation is rapamycin insensitive.** CNS stem cells were grown to medium or high local density before treatment. (A–E) Dense core of E14.5 cortical stem cell colonies after treatment and immunostaining for GFAP. (A) Simple withdrawal of bFGF (control) yields glia with immature morphology. (B) Treatment with CNTF before mitogen withdrawal yields CNS astrocytes with mature morphology. (C) Treatment with BMP4 before mitogen withdrawal yields glia with more flattened morphology. (D) Cotreatment with rapamycin blocks BMP4-mediated glial differentiation. (E) Cotreatment with FK506 has no effect on BMP4-mediated glial differentiation. (F and G) Quantitation of GFAP and SMA staining at the transitional zones in (F) medium-size/density E14.5 colonies, (G) large, high-density E14.5 colonies, and (H) medium-size/density adult colonies. Rectangles in cartoon colonies mark transitional zones chosen for quantitation; note that these zones have sizeable numbers of $GFAP^-SMA^-$ cells. Mean $GFAP^+$ or SMA^+ cells as percentage of total cells ± SEM (n = 6–9). Bar, 100 μm.

clones (Fig. 6, F and G). Rapamycin treatment caused a fourfold reduction in the generation of glia but had no significant effect on the number of smooth muscle cells. However, the number of $GFAP^{-}SMA^{-}$ or $GFAP^{low}SMA^{low}$ cells with a transitional morphology was increased, and there remained large numbers of SMA^{+} cells in the periphery. In all conditions, there was no observable cell death up to the time of fixation (4 d after withdrawal), indicating that the effect of treatment on gliogenesis was not the result of negative selection.

We then looked at the effect of rapamycin in adult stem cells. These cells are multipotent based on clonal assays (Johe et al., 1996), but BMP treatment promotes efficient glial differentiation even at lower densities that would promote smooth muscle differentiation in fetal stem cells. In these cells, rapamycin treatment caused a twofold reduction in the generation of glia and caused a twofold increase in the number of smooth muscle cells (Fig. 6 H). Thus, inhibition of FRAP specifically blocks the glial fate in both fetal and adult stem cells and redirects adult stem cells to a smooth muscle fate. These results are all consistent with the conclusion that BMP4 causes glial differentiation by FRAP-mediated Stat3 activation and smooth muscle differentiation by a FRAP-independent, SMAD-mediated mechanism.

BMP4 and CNTF have additive effects on glial differentiation

CNTF and BMPs both cause STAT activation and glial differentiation but do so by using different kinases. CNTF predominantly activates the janus kinases (Kisseleva et al., 2002), whereas we show that BMPs require a density-dependent signal in addition to FRAP (Fig. 5). Because distinct pathways are used to activate STAT proteins and cause glial differentiation, the simultaneous treatment of stem cells with both ligands might accelerate glial differentiation. Stem cells were plated at a medium density and treated with either ligand alone or together. As measured by GFAP expression, 25% of stem cells were differentiated by 24 h after CNTF treatment, whereas 50% of stem cells differentiated after 48 h. Cotreatment with BMP4 and CNTF increased glia number from 25 to 60% at 24 h and from 50 to 85% at 48 h (Fig. 7 A).

We then measured the effect of rapamycin during BMP4/CNTF cotreatment, hypothesizing that this would selectively inhibit BMP-mediated glial differentiation. As expected, rapamycin treatment abolished the additive effects that BMP4 lends to CNTF-mediated differentiation. A dose response of rapamycin shows that the effect is maximal at 1 μM (Fig. 7 B); no toxicity was observed at this dose, although higher doses led to cell death. In contrast, FK506 treatment had no effect on the accelerated differentiation by BMP4 and CNTF (Fig. 7 C). As BMP4 alone eventually induced most high-density stem cells to differentiate to the glial fate, combined treatment with BMP4 and CNTF appeared to affect the rate of glial differentiation rather than the final number of glia. Thus, distinct BMP and CNTF cytoplasmic signaling pathways converge through STAT proteins to promote glial differentiation.

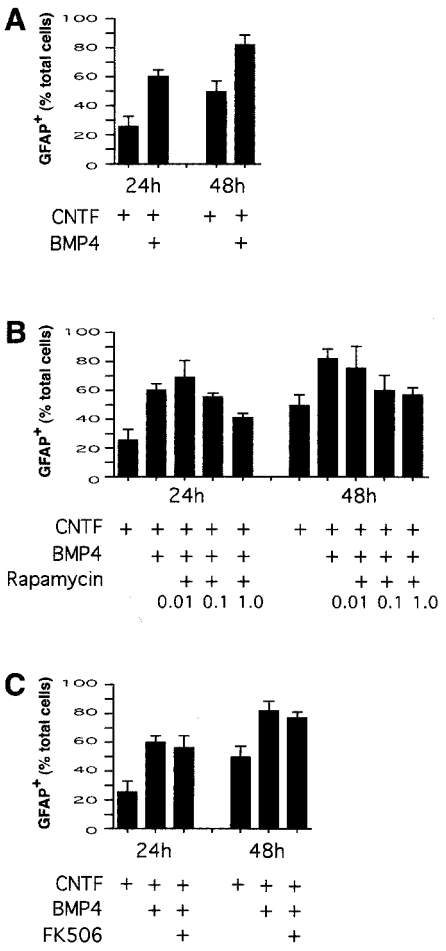

Figure 7. **BMP4 augments CNTF-mediated glial differentiation of CNS stem cells.** (A) Cells were treated with bFGF + CNTF (10 ng/ml) for 24 or 48 h and stained with anti-GFAP to measure glial differentiation. Where indicated, cells were treated with BMP4 for 4 h before CNTF treatment. BMP4 augments the effect of CNTF in generating glia at both 24 and 48 h of treatment. (B) Rapamycin blocks this augmentation in a dose-dependent manner (doses in μM). (C) Using FK506 (10 nM) instead of rapamycin does not affect the BMP-mediated augmentation of glial differentiation. Mean $GFAP^{+}$ cells as percentage of total cells ± SEM, $n = 4$.

Discussion

Combinatorial signals and fate choice

Stem cells can generate a number of distinct fates in response to BMPs, depending on the context in which BMP signaling is received. In this study, we use a defined and homogeneous neural stem cell culture to show that BMP4 efficiently induces the generation of smooth muscle and glia in a density-dependent manner. We further show that BMP4 activates two distinct cytoplasmic signaling pathways in stem cells, one mediated by SMAD proteins and the other by STAT proteins. In low-density cultures with low basal levels of activated STAT proteins, BMP4 induces smooth muscle differentiation by activating Smad1/5/8. In high-density cultures that show higher basal levels of activated STAT proteins, BMP4 further activates STAT proteins to generate glia at the expense of smooth muscle. The activation of STAT proteins by BMP4 involves a novel pathway

mediated by the serine-threonine kinase FRAP. This provides strong evidence that FRAP and STAT proteins are part of a newly described signal transduction pathway available in response to BMPs.

Our results show that fate choice decisions leading to glial or nonglial fates downstream of BMPs can be made in the cytoplasm. This provides a novel complement to previous studies showing that glial differentiation in response to BMPs is regulated in the nucleus. In these studies, glial differentiation requires the coactivators cyclic AMP response element–binding protein (CBP)/p300 in a complex with STAT and SMAD proteins (Nakashima et al., 1999). The differentiation of glia by either BMPs or CNTF is inhibited by the basic helix-loop-helix protein neurogenin1, which acts in part by sequestering the CBP–Smad1 complex from association with STAT proteins. In CNS stem cells expressing high levels of neurogenin1, BMPs induce neuronal, rather than glial, differentiation (Sun et al., 2001). Our results show that glial versus nonglial fates can also be regulated by alternative cytoplasmic signals. These alternative pathways are subject to control by density-dependent signals, consistent with our previous findings (Tsai and McKay, 2000). Whereas BMP4 activates SMADs at both low and high densities, its activation of Stat3 at high density results in glial differentiation regardless of SMAD activation (Table II; Figs. 2 and 3). Furthermore, glial differentiation can occur even when SMAD signaling is inhibited (Table II). One interpretation of this result is that sufficiently high levels of STAT activation promote glial differentiation without the requirement for SMADs. Alternatively, SMAD activation may modify the type of glia that is generated, as evidenced by the morphological difference in glia generated from CNTF- versus BMP-treated stem cells (Figs. 6 and 7).

In addition to density-dependent biases, stem cells also exhibit age-dependent biases in fate choice that mirror the in vivo developmental progression of cell type differentiation. Activating BMP signals in vivo results in apoptosis in early gestation precursors and neurogenesis in midgestation precursors (Panchision et al., 2001). Similarly, neural stem cells isolated from progressively older embryos respond to BMPs first with apoptosis, and then with neuronal and finally glial differentiation (Gross et al., 1996; Mabie et al., 1999). Our FRAP inhibition experiments suggest that the same mechanisms for glial differentiation are accessible in both fetal and adult stem cells and that age-intrinsic differences between stem cells can be reversible (Fig. 6).

Previous studies have shown that the same signaling molecules can promote either stem cell self-renewal or gliogenesis. Notch activation is required for the maintenance of early gestation neural stem cells (Hitoshi et al., 2002a) but also promotes gliogenesis in stem cells from older embryos (Tanigaki et al., 2001; White et al., 2001). Stat3, which we show to be activated by BMPs through FRAP, has been shown to promote both glial differentiation in neural stem cells (Bonni et al., 1997; Rajan and McKay, 1998) and self-renewal of embryonic stem cells (Niwa et al., 1998; Nishinakamura et al., 1999; Boeuf et al., 2001) in response to CNTF or Leukemia inhibitory factor. FRAP signaling is required for proliferation in mouse embryos and the loss-of-function phenotype is mimicked by the treatment of embryos with rapamycin (Hentges et al., 2001). Our results show a novel pathway in which FRAP is recruited to promote gliogenesis by activating Stat3. Presumably this is due to other signals that provide a different context to FRAP and STAT signaling, but the mechanisms that mediate this changing context remain to be identified. In our in vitro stem cell system, this potentially translates into a density-mediated signal. Our results add FRAP to a growing list of signaling molecules whose actions are redirected from self-renewal/proliferation to gliogenesis during development.

A novel mechanism for signal integration

Our results suggest that the immunophilin FKBP12 is involved in glial differentiation, but its exact role is unclear. FKBP12 binds TGFβ receptors (Wang et al., 1996) and inhibits the basal activity of the receptor in the absence of ligand (Chen et al., 1997). We show that FKBP12 complexes with BMPR-IA in stem cells and is released upon binding of BMP4 to its receptor (Fig. 5). The timing of the release of FKBP12 from the BMP receptor correlates with activation of Stat3 (~6 h), suggesting that FKBP12 is also involved in the kinetics of FRAP activation. FKBP12 can complex with the antibiotic drugs FK506 and rapamycin to inhibit distinct signaling pathways. FK506 binding to FKBP12 inhibits the activity of calcineurin in T cells, causing immunosuppression (Clipstone et al., 1994), whereas rapamycin binding to FKBP12 inhibits the activation of FRAP (Hamilton and Steiner, 1998). We show that rapamycin, but not FK506, specifically inhibits the BMP-mediated augmentation of Stat3 activation and glial differentiation (Fig. 6). It is important to note that all our studies are performed with endogenous cellular proteins, with the exception of dominant-negative inhibitory proteins that we have overexpressed. This, and the fact that our cultures are dynamically undergoing differentiation, may allow us to speculate on novel functions for FKBP12. We could not isolate a complex of FKBP12 and FRAP in BMP-treated cells (unpublished data), in agreement with a previous crystallographic analysis showing that FKBP12 does not bind directly to FRAP (Choi et al., 1996). FKBP12 may complex with other proteins, or be modified, as it is released from the receptor. The intrinsic peptidyl-prolyl isomerase activity (Siekierka et al., 1990) may be significant in these signaling interactions. The region of FRAP required for binding to FKBP12–rapamycin complex is also required for the activation of its serine-threonine kinase activity (Vilella-Bach et al., 1999). This may suggest an endogenous cellular analogue of rapamycin that functions in FKBP12-mediated activation of FRAP. However, we cannot discount the likelihood that FKBP12 is acting strictly as an inhibitor of both BMP receptor and FRAP activity, so the signaling molecules linking BMP receptor activation with FRAP activation remain undetermined.

The serine-threonine kinase FRAP is an important regulator of cell growth and proliferation (Hentges et al., 2001; Fingar et al., 2002). FRAP acts by promoting the synthesis of proteins crucial to increasing cell size and to cell cycle progression (Gingras et al., 2001; Fingar et al., 2002). FRAP activity is nutrient dependent and increases with rising amino acid levels and insulin signaling (Gingras et al.,

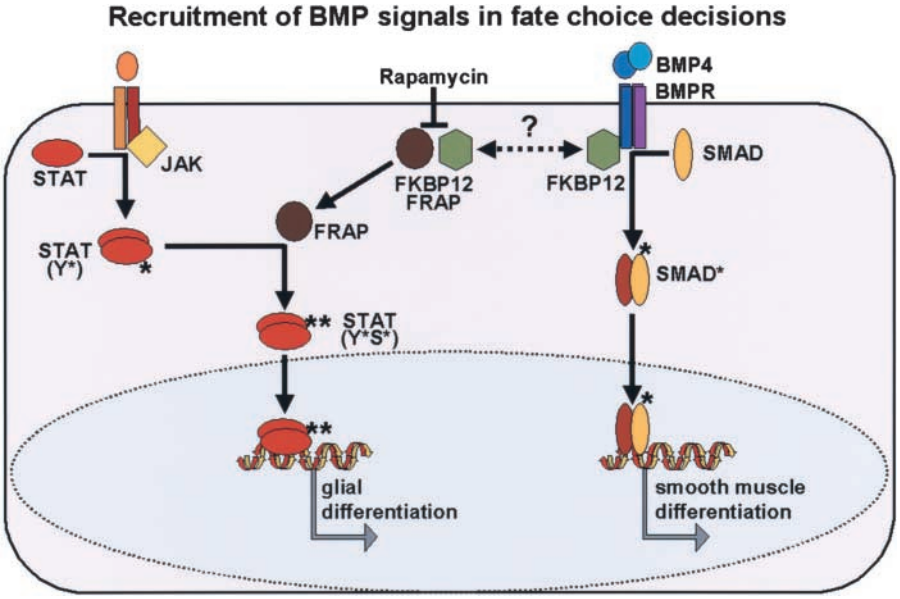

Figure 8. **Model for recruitment of BMP signals in fate choice decisions.** BMP4 causes the activation of at least two signaling pathways in neural stem cells. Upon ligand–receptor binding, the BMPR receptor complex releases FKBP12 and activates SMAD proteins, resulting in smooth muscle differentiation. The released FKBP12 may bind with rapamycin to inhibit FRAP or may act in some modified form to activate FRAP. FRAP then catalyzes serine phosphorylation (S*) of STAT to augment its prior activation by tyrosine phosphorylation (Y*) by another signal. High cell density (described in text) acts to promote basal STAT activation and DNA binding by an unknown signaling mechanism. This enhanced activation of STAT (Y*S*) causes efficient glial differentiation. Levels of activated STAT proteins in the cell dictate whether the STAT or SMAD signal acquires precedence in the fate choice between smooth muscle and glia.

2001). One possibility is that rapamycin may mimic an endogenous inhibitor of otherwise constitutively active FRAP (Gingras et al., 2001). Overexpressed FRAP causes Stat3 phosphorylation at serine residue 727 (Yokogami et al., 2000). This suggests a model where BMPs, by causing serine phosphorylation of STAT proteins, can integrate with other signals that tyrosine phosphorylate STAT proteins; this concerted action would raise STAT activation above a threshold required for differentiation to the glial fate and would override a SMAD protein–mediated smooth muscle fate (Fig. 8).

A number of recent studies show that stem cells from many tissues can adopt a broad range of unexpected fates (Valtz et al., 1991; Bjornson et al., 1999; Gussoni et al., 1999; Jackson et al., 1999; Galli et al., 2000; Lagasse et al., 2000). However, these results beg the question of how extrinsic signals can control cell fate in such unexpected ways. This study, along with our previous results (Tsai and McKay, 2000; Panchision et al., 2001), demonstrate that defined pathways remain accessible to stem cells throughout development. As there is increasing evidence that stem cells continuously monitor morphogenic signals to make decisions regarding identity and self-renewal (Hitoshi et al., 2002b; Panchision and McKay, 2002), these fate-choice mechanisms have increasing importance for understanding development as well as designing therapeutic treatments.

Materials and methods

Materials

All tissue culture reagents were obtained as previously described (Johe et al., 1996; Rajan and McKay, 1998).

Antibodies. The following antibodies were used: monoclonal anti-GFAP from ICN Biomedicals; polyclonal anti-GFAP from DakoCytomation; monoclonal anti-SMA and anti-FLAG from Sigma-Aldrich; polyclonal anti-HA from BABCO; monoclonal anti-FKBP12, anti-FRAP, and anti-Stat3 from Transduction Laboratories; polyclonal anti-phosphoStat3 (Tyr705 and Ser727) from Santa Cruz Biotechnology, Inc.; monoclonal anti–BMPR-IA from R&D Systems; polyclonal anti-phosphoSmad1/5/8 (a gift of P. ten Dijke, Netherlands Cancer Institute, Amsterdam, Netherlands; or purchased from Cell Signaling); fluorescent-labeled secondary antibodies from Jackson ImmunoResearch Laboratories; and peroxidase-conjugated secondaries for ECL from Boehringer.

Other reagents. Other reagents included ECL reagents from Pierce Chemical Co., polyacrylamide gradient gels from Novex, protein A–Sepharose from Amersham Biosciences, Ponceau S from Sigma-Aldrich, Lipofectamine Plus from Invitrogen, rapamycin and α-amanitin from Calbiochem, FK506 from American Qualex, and BMP2 and BMP4 from Genetics Institute.

Plasmids. The Stat3 mutant (a gift from J.E. Darnell, The Rockefeller University, New York, NY) has a three amino acid substitution in the DNA binding domain as previously described (Horvath et al., 1995) and was tagged with a synthetic FLAG epitope. The Smad7 construct (a gift from P. ten Dijke, Netherlands Cancer Institute, Amsterdam, Netherlands) (Ishisaki et al., 1999) was modified such that it expressed the protein with an NH_2-terminal HA epitope under the control of the β-actin promoter (a gift from J. Rossant, Children's Hospital, Toronto, Canada). The kinase-dead FRAP construct has a Trp2027 to Phe inactivating mutation in the kinase domain (Vilella-Bach et al., 1999). The FRB-defective FRAP construct has an Asp2357 to Glu mutation that prevents protein interactions via the FRB domain (Vilella-Bach et al., 1999). Both FLAG constructs (gifts from J. Chen, University of Illinois, Urbana-Champaign, IL) were tagged with an NH_2-terminal synthetic FLAG epitope.

Cell culture and treatments

Embryonic and adult rat stem cells were grown as previously described (Johe et al., 1996; Rajan and McKay, 1998). To grow adult stem cells, ventricular and subventricular tissue was dissected from the brains of young adult female rats (200–250 g weight), enzymatically dissociated, and plated in serum-free DME/F12 medium with N2 supplement. bFGF was included at 10 ng/ml to promote rat stem cell proliferation. Stem cells from E13 mouse cortex were required for one experiment using a mouse-specific Stat3 (pSer727) antibody and were grown as described for rat, except mouse cells were incubated in 5% oxygen and 20 ng/ml bFGF. Cells were fed with bFGF daily, and medium was replaced on alternate days during stem cell expansion. Passaging was performed nonenzymatically using Ca^{2+}/Mg^{2+}-free HBSS. All experiments were performed on first- or second-passage cells.

For mass culture experiments, cells were plated at 7,000 cells/cm^2 and BMP treatment was initiated after 1 d (low density) or 4 d (high density). Alternatively, cells were plated at 350 cells/cm^2 and BMP treatment was initiated immediately (low density) or after 4 d (high density). For clonal analysis, cells were plated at 35 cells/cm^2 and BMP treatment was initiated immediately (low density) or after 6 d (high density). BMP4 was added daily, usually for 2 d in the presence of bFGF and for another 4 d after bFGF withdrawal to promote efficient terminal differentiation of stem cells.

Drug inhibition experiments were performed using the 350 cells/cm^2 plating paradigm described above. When needed, CNTF (10 ng/ml), rapa-

mycin (1 μM), or FK506 (1 μg/ml) were used in the same manner as BMP4. Separate experiments involving BMP/CNTF cotreatment were performed using the 7,000 cells/cm^2 plating paradigm; cells were treated with BMP4 for 3 d in the presence of bFGF and for another 3 d in the absence of bFGF.

For the biochemical assays, cells were treated with factors and harvested at the time points mentioned in the figure legends. For transcriptional inhibition experiments, cells were preincubated with α-amanitin (5 μg/ml) for 20 min before and along with BMP treatment before harvesting of cells. Transfections were performed with Lipofectamine Plus reagent according to the manufacturer's instructions (Invitrogen). For Stat3 and Smad7 manipulations, cells were plated at 3,500 cells/cm^2 and cultured with 10 ng/ml bFGF for 1 d before transfection and for 3 d after transfection to allow the dominant-negative Stat3–FLAG or Smad7–HA plasmid to express before BMP4 treatment. Cells were then treated with 10 ng/ml BMP4 for 3 d with bFGF mitogen and for 3 d after mitogen withdrawal. For FRAP manipulations, cells were plated at 350 cells/cm^2 and cultured with 10 ng/ml bFGF for 4 d before transfection and for 1 d after transfection to allow the kinase-dead or FRB-defective FRAP plasmid to express before BMP4 treatment. The transfection efficiency was ~10%, as measured by epitope tag staining.

Immunofluorescent staining of cells

Cells were fixed with 4% paraformaldehyde for 10–15 min at room temperature, blocked for 30 min in PBS with 0.1% triton and 5% normal goat serum, and incubated with the primary antibody for 2–4 h at room temperature. Cells were stained as directed with anti-SMA to detect smooth muscle cells and anti-GFAP to detect glia. After two washes in PBS, the secondary antibody was applied at a 100-fold dilution for 1 h at room temperature. Cultures were then washed with PBS and mounted in Vectashield containing DAPI (Vector Laboratories). Images were photographed under fluorescent filters using a Carl Zeiss MicroImaging, Inc. Axioplan microscope and Spot digital camera (Diagnostic Instruments, Inc.). Statistical analysis and histogram illustration of cell numbers were performed using SigmaPlot 5.0 (SPSS, Inc.). Other graphic illustrations were generated using Powerpoint for Windows (Microsoft). All images were combined for figures using Adobe Photoshop 5.0® for Windows.

EMSA

Nuclear extract preparation and EMSA were performed as described previously (Rajan and McKay, 1998). Autoradiography was performed using Biomax M_r film (Eastman Kodak Co.), and images were digitally imported using a Duoscan T2500 flatbed scanner (AGFA) and processed for figures using Adobe Photoshop 5.0® for Windows.

Immunoprecipitation and immunoblotting

Total cell lysates were prepared in nondenaturing lysis buffer (1% Triton X-100, 10% glycerol, 50 mM Tris, pH 7.4, 150 mM NaCl, 2 mM EGTA, 2 mM $MgCl_2$, 1 mM DTT, 1 mM PMSF, and phosphatase inhibitors) and were normalized for protein concentration. For immunoprecipitation, normalized lysates were incubated with primary antibody overnight at 4°C. After incubation with protein A–Sepharose (1:1 vol/vol), the immune complexes were washed twice with PBS and heated to 70°C in SDS-PAGE loading buffer. Samples were resolved in denaturing gels and transferred onto nitrocellulose. Filters were blocked overnight in Tris-buffered saline (20 mM Tris, pH 7.6, 137 mM NaCl) with 0.1% Tween 20 (TBST) containing 3% bovine serum albumin. Filters were incubated with primary antibody (1:1,000 dilution in blocking buffer) for 4 h at room temperature and then washed three times in TBST for 1 h. Filters were then incubated with the appropriate secondary antibody (1:20,000 dilution in blocking buffer) for 1 h and then washed for 1 h. Relevant bands were detected with ECL according to the manufacturer's instructions. Ponceau S staining (0.1% in 5% acetic acid) was performed for 30 s, followed by destaining in several changes of purified water. Banding patterns were digitally scanned as described above.

BMP2 and BMP4 were obtained by agreement with Genetics Institute.

L. Newell is funded by the Howard Hughes Medical Institute National Institutes of Health Research Scholar's Program.

Submitted: 5 November 2002
Revised: 23 April 2003
Accepted: 23 April 2003

References

Abraham, R.T., and G.J. Wiederrecht. 1996. Immunopharmacology of rapamycin. *Annu. Rev. Immunol.* 14:483–510.

Bjornson, C.R., R.L. Rietze, B.A. Reynolds, M.C. Magli, and A.L. Vescovi. 1999. Turning brain into blood: a hematopoietic fate adopted by adult neural stem cells in vivo. *Science.* 283:534–537.

Boeuf, H., K. Merienne, S. Jacquot, D. Duval, M. Zeniou, C. Hauss, B. Reinhardt, Y. Huss-Garcia, A. Dierich, D.A. Frank, et al. 2001. The ribosomal S6 kinases, cAMP-responsive element-binding, and STAT3 proteins are regulated by different leukemia inhibitory factor signaling pathways in mouse embryonic stem cells. *J. Biol. Chem.* 276:46204–46211.

Bonni, A., Y. Sun, M. Nadal-Vicens, A. Bhatt, D.A. Frank, I. Rozovsky, N. Stahl, G.D. Yancopoulos, and M.E. Greenberg. 1997. Regulation of gliogenesis in the central nervous system by the JAK-STAT signaling pathway. *Science.* 278:477–483.

Chen, Y.G., F. Liu, and J. Massague. 1997. Mechanism of TGFβ receptor inhibition by FKBP12. *EMBO J.* 16:3866–3876.

Choi, J., J. Chen, S.L. Schreiber, and J. Clardy. 1996. Structure of the FKBP12–rapamycin complex interacting with the binding domain of human FRAP. *Science.* 273:239–242.

Clipstone, N.A., D.F. Fiorentino, and G.R. Crabtree. 1994. Molecular analysis of the interaction of calcineurin with drug-immunophilin complexes. *J. Biol. Chem.* 269:26431–26437.

Dorsky, R.I., R.T. Moon, and D.W. Raible. 2000. Environmental signals and cell fate specification in premigratory neural crest. *Bioessays.* 22:708–716.

Faure, S., M.A. Lee, T. Keller, P. ten Dijke, and M. Whitman. 2000. Endogenous patterns of TGFβ superfamily signaling during early *Xenopus* development. *Development.* 127:2917–2931.

Fingar, D.C., S. Salama, C. Tsou, E. Harlow, and J. Blenis. 2002. Mammalian cell size is controlled by mTOR and its downstream targets S6K1 and 4EBP1/eIF4E. *Genes Dev.* 16:1472–1487.

Furuta, Y., D.W. Piston, and B.L. Hogan. 1997. Bone morphogenetic proteins (BMPs) as regulators of dorsal forebrain development. *Development.* 124:2203–2212.

Galli, R., U. Borello, A. Gritti, M.G. Minasi, C. Bjornson, M. Coletta, M. Mora, M.G. De Angelis, R. Fiocco, G. Cossu, and A.L. Vescovi. 2000. Skeletal myogenic potential of human and mouse neural stem cells. *Nat. Neurosci.* 3:986–991.

Gingras, A.C., B. Raught, and N. Sonenberg. 2001. Regulation of translation initiation by FRAP/mTOR. *Genes Dev.* 15:807–826.

Graham, A., G. Koentges, and A. Lumsden. 1996. Neural crest apoptosis and the establishment of craniofacial pattern: an honorable death. *Mol. Cell. Neurosci.* 8:76–83.

Gross, R.E., M.F. Mehler, P.C. Mabie, Z. Zang, L. Santschi, and J.A. Kessler. 1996. Bone morphogenetic proteins promote astroglial lineage commitment by mammalian subventricular zone progenitor cells. *Neuron.* 17:595–606.

Gussoni, E., Y. Soneoka, C.D. Strickland, E.A. Buzney, M.K. Khan, A.F. Flint, L.M. Kunkel, and R.C. Mulligan. 1999. Dystrophin expression in the mdx mouse restored by stem cell transplantation. *Nature.* 401:390–394.

Hamilton, G.S., and J.P. Steiner. 1998. Immunophilins: beyond immunosuppression. *J. Med. Chem.* 41:5119–5143.

Hentges, K.E., B. Sirry, A.C. Gingeras, D. Sarbassov, N. Sonenberg, D. Sabatini, and A.S. Peterson. 2001. FRAP/mTOR is required for proliferation and patterning during embryonic development in the mouse. *Proc. Natl. Acad. Sci. USA.* 98:13796–13801.

Hitoshi, S., T. Alexson, V. Tropepe, D. Donoviel, A.J. Elia, J.S. Nye, R.A. Conlon, T.W. Mak, A. Bernstein, and D. van der Kooy. 2002a. Notch pathway molecules are essential for the maintenance, but not the generation, of mammalian neural stem cells. *Genes Dev.* 16:846–858.

Hitoshi, S., V. Tropepe, M. Ekker, and D. van der Kooy. 2002b. Neural stem cell lineages are regionally specified, but not committed, within distinct compartments of the developing brain. *Development.* 129:233–244.

Horvath, C.M., Z. Wen, and J.E. Darnell. 1995. A STAT protein domain that determines DNA sequence recognition suggests a novel DNA-binding domain. *Genes Dev.* 9:984–994.

Ishisaki, A., K. Yamato, S. Hashimoto, A. Nakao, K. Tamaki, K. Nonaka, P. ten Dijke, H. Sugino, and T. Nishihara. 1999. Differential inhibition of Smad6 and Smad7 on bone morphogenetic protein- and activin-mediated growth arrest and apoptosis in B cells. *J. Biol. Chem.* 274:13637–13642.

Jackson, K.A., T. Mi, and M.A. Goodell. 1999. Hematopoietic potential of stem cells isolated from murine skeletal muscle. *Proc. Natl. Acad. Sci. USA.* 96:14482–14486.

Johe, K.K., T.G. Hazel, T. Muller, M.M. Dugich-Djordjevic, and R.D. McKay. 1996. Single factors direct the differentiation of stem cells from the fetal and adult central nervous system. *Genes Dev.* 10:3129–3140.

Kisseleva, T., S. Bhattacharya, J. Braunstein, and C.W. Schindler. 2002. Signaling

through the JAK/STAT pathway, recent advances and future challenges. *Gene.* 285:1–24.

Kuruvilla, F.G., and S.L. Schreiber. 1999. The PIK-related kinases intercept conventional signaling pathways. *Chem. Biol.* 6:R129–R136.

Lagasse, E., H. Connors, M. Al-Dhalimy, M. Reitsma, M. Dohse, L. Osborne, X. Wang, M. Finegold, I.L. Weissman, and M. Grompe. 2000. Purified hematopoietic stem cells can differentiate into hepatocytes in vivo. *Nat. Med.* 6:1229–1234.

Li, W., C.A. Cogswell, and J.J. LoTurco. 1998. Neuronal differentiation of precursors in the neocortical ventricular zone is triggered by BMP. *J. Neurosci.* 18: 8853–8862.

Liem, K.F.J., G. Tremml, and T.M. Jessell. 1997. A role for the roof plate and its resident TGFβ-related proteins in neuronal patterning in the dorsal spinal cord. *Cell.* 91:127–138.

Mabie, P.C., M.F. Mehler, and J.A. Kessler. 1999. Multiple roles of bone morphogenetic protein signaling in the regulation of cortical cell number and phenotype. *J. Neurosci.* 19:7077–7088.

Miyazono, K. 1999. Signal transduction by bone morphogenetic protein receptors: functional roles of Smad proteins. *Bone.* 25:91–93.

Molne, M., L. Studer, V. Tabar, Y.T. Ting, M.V. Eiden, and R.D. McKay. 2000. Early cortical precursors do not undergo LIF-mediated astrocytic differentiation. *J. Neurosci. Res.* 59:301–311.

Mujtaba, T., M. Mayer-Proschel, and M.S. Rao. 1998. A common neural progenitor for the CNS and PNS. *Dev. Biol.* 200:1–15.

Nakashima, K., M. Yanagisawa, H. Arakawa, N. Kimura, T. Hisatsune, M. Kawabata, K. Miyazono, and T. Taga. 1999. Synergistic signaling in fetal brain by STAT3-Smad1 complex bridged by p300. *Science.* 284:479–482.

Nishinakamura, R., Y. Matsumoto, T. Matsuda, T. Ariizumi, T. Heike, M. Asashima, and T. Yokota. 1999. Activation of Stat3 by cytokine receptor gp130 ventralizes *Xenopus* embryos independent of BMP-4. *Dev. Biol.* 216:481–490.

Niwa, H., T. Burdon, I. Chambers, and A. Smith. 1998. Self-renewal of pluripotent embryonic stem cells is mediated via activation of STAT3. *Genes Dev.* 12:2048–2060.

Panchision, D.M., and R.D. McKay. 2002. The control of neural stem cells by morphogenic signals. *Curr. Opin. Genet. Dev.* 12:478–487.

Panchision, D.M., J.M. Pickel, L. Studer, S.H. Lee, P.A. Turner, T.G. Hazel, and R.D. McKay. 2001. Sequential actions of BMP receptors control neural precursor cell production and fate. *Genes Dev.* 15:2094–2110.

Rajan, P., and R.D. McKay. 1998. Multiple routes to astrocytic differentiation in the CNS. *J. Neurosci.* 18:3620–3629.

Sela-Donenfeld, D., and C. Kalcheim. 1999. Regulation of the onset of neural crest migration by coordinated activity of BMP4 and Noggin in the dorsal neural tube. *Development.* 126:4749–4762.

Shah, N.M., A.K. Groves, and D.J. Anderson. 1996. Alternative neural crest cell fates are instructively promoted by TGFβ superfamily members. *Cell.* 85: 331–343.

Siekierka, J.J., G. Wiederrecht, H. Greulich, D. Boulton, S.H. Hung, J. Cryan, P.J. Hodges, and N.H. Sigal. 1990. The cytosolic-binding protein for the immunosuppressant FK-506 is both a ubiquitous and highly conserved peptidyl-prolyl cis-trans isomerase. *J. Biol. Chem.* 265:21011–21015.

Souchelnytskyi, S., T. Nakayama, A. Nakao, A. Moren, C.H. Heldin, J.L. Christian, and P. ten Dijke. 1998. Physical and functional interaction of murine and *Xenopus* Smad7 with bone morphogenetic protein receptors and transforming growth factor-β receptors. *J. Biol. Chem.* 273:25364–25370.

Stockwell, B.R., and S.L. Schreiber. 1998. TGFβ-signaling with small molecule FKBP12 antagonists that bind myristoylated FKBP12-TGFβ type I receptor fusion proteins. *Chem. Biol.* 5:385–395.

Sun, Y., M. Nadal-Vicens, S. Misono, M.Z. Lin, A. Zubiaga, X. Hua, G. Fan, and M.E. Greenberg. 2001. Neurogenin promotes neurogenesis and inhibits glial differentiation by independent mechanisms. *Cell.* 104:365–376.

Tanigaki, K., F. Nogaki, J. Takahashi, K. Tashiro, H. Kurooka, and T. Honjo. 2001. Notch1 and Notch3 instructively restrict bFGF-responsive multipotent neural progenitor cells to an astroglial fate. *Neuron.* 29:45–55.

Tsai, R.Y., and R.D. McKay. 2000. Cell contact regulates fate choice by cortical stem cells. *J. Neurosci.* 20:3725–3735.

Valtz, N.L., T.E. Hayes, T. Norregaard, S.M. Liu, and R.D. McKay. 1991. An embryonic origin for medulloblastoma. *New Biol.* 3:364–371.

Vicario-Abejon, C., K.K. Johe, T.G. Hazel, D. Collazo, and R.D. McKay. 1995. Functions of basic fibroblast growth factor and neurotrophins in the differentiation of hippocampal neurons. *Neuron.* 15:105–114.

Vilella-Bach, M., P. Nuzzi, Y. Fang, and J. Chen. 1999. The FKBP12-rapamycin-binding domain is required for FKBP12-rapamycin-associated protein kinase activity and G1 progression. *J. Biol. Chem.* 274:4266–4272.

Wang, T., B.Y. Li, P.D. Danielson, P.C. Shah, S. Rockwell, R.J. Lechleider, J. Martin, T. Manganaro, and P.K. Donahoe. 1996. The immunophilin FKBP12 functions as a common inhibitor of the TGFβ family type I receptors. *Cell.* 86:435–444.

White, P.M., S.J. Morrison, K. Orimoto, C.J. Kubu, J.M. Verdi, and D.J. Anderson. 2001. Neural crest stem cells undergo cell-intrinsic developmental changes in sensitivity to instructive differentiation signals. *Neuron.* 29:57–71.

Wieland, T., and H. Faulstich. 1978. Amatoxins, phallotoxins, phallolysin, and antamanide: the biologically active components of poisonous Amanita mushrooms. *CRC Crit. Rev. Biochem.* 5:185–260.

Yokogami, K., S. Wakisaka, J. Avruch, and S.A. Reeves. 2000. Serine phosphorylation and maximal activation of STAT3 during CNTF signaling is mediated by the rapamycin target mTOR. *Curr. Biol.* 10:47–50.

Zhang, X., J. Blenis, H.C. Li, C. Schindler, and S. Chen-Kiang. 1995. Requirement of serine phosphorylation for formation of STAT-promoter complexes. *Science.* 267:1990–1994.

Zhu, J., and S.G. Emerson. 2002. Hematopoietic cytokines, transcription factors and lineage commitment. *Oncogene.* 21:3295–3313.